

Dynamics of a delay limit cycle oscillator with self-feedback

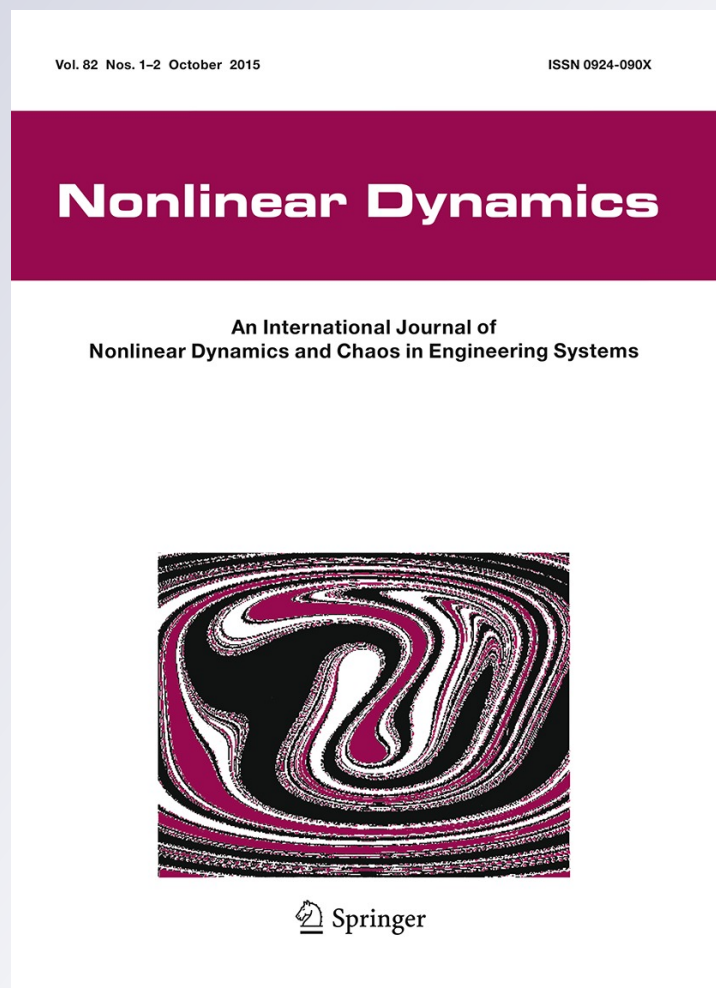
Lauren Lazarus, Matthew Davidow & Richard Rand

Nonlinear Dynamics

An International Journal of Nonlinear Dynamics and Chaos in Engineering Systems

ISSN 0924-090X
Volume 82
Combined 1-2

Nonlinear Dyn (2015) 82:481-488
DOI 10.1007/s11071-015-2169-z



Your article is protected by copyright and all rights are held exclusively by Springer Science +Business Media Dordrecht. This e-offprint is for personal use only and shall not be self-archived in electronic repositories. If you wish to self-archive your article, please use the accepted manuscript version for posting on your own website. You may further deposit the accepted manuscript version in any repository, provided it is only made publicly available 12 months after official publication or later and provided acknowledgement is given to the original source of publication and a link is inserted to the published article on Springer's website. The link must be accompanied by the following text: "The final publication is available at link.springer.com".

Dynamics of a delay limit cycle oscillator with self-feedback

Lauren Lazarus · Matthew Davidow ·
Richard Rand

Received: 21 October 2014 / Accepted: 15 May 2015 / Published online: 28 May 2015
 © Springer Science+Business Media Dordrecht 2015

Abstract This paper concerns the dynamics of the following nonlinear differential-delay equation: $\dot{x} = -x(t - T) - x^3 + \alpha x$ in which T is the delay and α is a coefficient of self-feedback. Using numerical integration, continuation programs and bifurcation theory, we show that this system exhibits a wide range of dynamical phenomena, including Hopf and pitchfork bifurcations, limit cycle folds and relaxation oscillations.

Keywords Differential-delay equation · Limit cycle · Hopf bifurcation

1 Introduction

Limit cycle oscillators have been of great interest to researchers in nonlinear dynamics ever since the time of Rayleigh [1] and van der Pol [2].

Recent interest in dynamical systems with delay has produced a new type of oscillator which has the form of a differential-delay equation (DDE):

L. Lazarus · R. Rand
 Department of Mechanical and Aerospace Engineering,
 Cornell University, Ithaca, NY, USA

M. Davidow
 Department of Applied and Engineering Physics,
 Cornell University, Ithaca, NY, USA

R. Rand (✉)
 Department of Mathematics, Cornell University, Ithaca,
 NY, USA
 e-mail: rhr2@cornell.edu

$$\dot{x} = -x(t - T) - x^3 \quad (1)$$

As we shall see, this system exhibits a Hopf bifurcation at $T = \pi/2$ in which a limit cycle is born [5,6]. We shall refer to Eq. (1) as a “delay limit cycle oscillator.”

Additionally, recent studies have been made of van der Pol oscillators with delayed self-feedback [3,4].

In this paper, we consider Eq. (1) with a self-feedback term:

$$\dot{x} = -x(t - T) - x^3 + \alpha x \quad (2)$$

Equation (2) may be described as a delay limit cycle oscillator with self-feedback.

2 Equilibria and their stability

Equilibria in Eq. (2) are given by the equation

$$0 = -x - x^3 + \alpha x \quad (3)$$

For $\alpha < 1$, only $x = 0$ is a solution. For $\alpha \geq 1$, an additional pair of solutions $x = \pm\sqrt{\alpha - 1}$ exist such that there are three constant solutions. These solutions emerge from the $x = 0$ solution in a pitchfork bifurcation at $\alpha = 1$.

In order to determine the stability of the equilibrium at $x = 0$, we investigate the linearized DDE:

$$\dot{x} = -x(t - T) + \alpha x \quad (4)$$

Setting $x = Ae^{\lambda t}$, we obtain the characteristic equation:

$$\lambda = -e^{-\lambda T} + \alpha \quad (5)$$

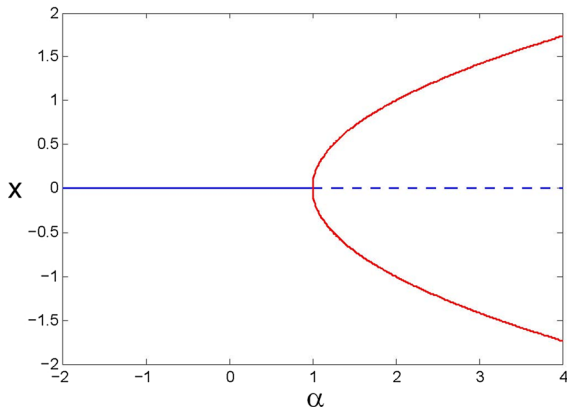


Fig. 1 Locations of equilibria as a function of α , independent of T

In the zero-delay ($T = 0$) case, we are left with $\lambda = \alpha - 1$; therefore, $x = 0$ is stable for $\alpha < 1$ and becomes unstable for $\alpha > 1$ where the other equilibria (the arms of the pitchfork) exist.

For nonzero delay ($T > 0$), we anticipate the existence of a Hopf bifurcation and the creation of a limit cycle, based on the known behavior for $\alpha = 0$. We look for pure imaginary eigenvalues by substituting $\lambda = i\omega$ into the characteristic Eq. (5) and separating the real and imaginary terms into separate equations:

$$\omega = \sin(\omega T) \tag{6}$$

$$0 = -\cos(\omega T) + \alpha \tag{7}$$

By manipulating these, we obtain:

$$\sin^2(\omega T) + \cos^2(\omega T) = \omega^2 + \alpha^2 = 1 \tag{8}$$

$$T_H = \frac{\arccos \alpha}{\omega} = \frac{\arccos \alpha}{\sqrt{1 - \alpha^2}} \tag{9}$$

So for a given α , there exists a delay T_H where a Hopf bifurcation occurs at $x = 0$. In this case, the Hopf bifurcations only exist for $-1 < \alpha < 1$, since real ω and finite T_H cannot exist otherwise. Note that for $\alpha = 0$ [which corresponds to the uncoupled oscillator of Eq. (1)], the Hopf occurs at $T_H = \pi/2$. Figure 2 shows the stability of the $x = 0$ equilibrium point in $\alpha - T$ space.

Next, we consider the stability of the equilibria located along the arms of the pitchfork at

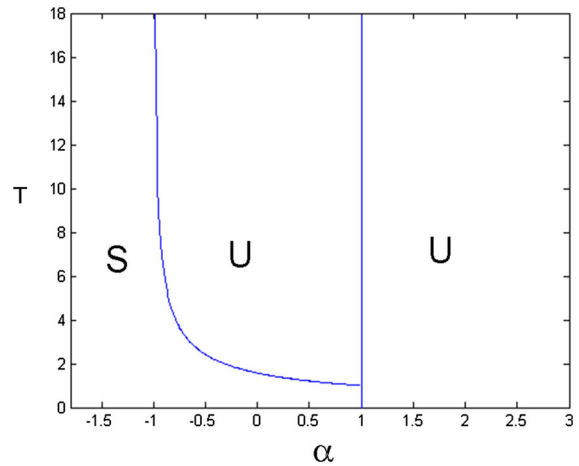


Fig. 2 Stability diagram for the equilibrium at $x = 0$. Regions are marked for the equilibria being stable (S) or unstable (U). The curved line is given by Hopf Eq. (9). The instability for $\alpha > 1$ is due to a pitchfork bifurcation

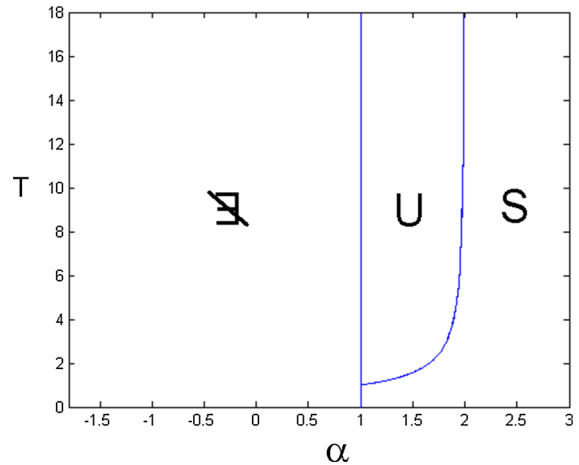


Fig. 3 Stability diagram for the equilibria at $x = \pm\sqrt{\alpha - 1}$. Regions are marked for the equilibria being nonexistent, unstable (U) or stable (S). The curved line is given by Hopf Eq. (13)

$$x = \pm\sqrt{\alpha - 1} \tag{10}$$

We begin by setting $x = \pm\sqrt{\alpha - 1} + z$ which gives the following nonlinear DDE:

$$\dot{z} = -z(t - T) + (3 - 2\alpha)z \mp 3\sqrt{\alpha - 1}z^2 - z^3 \tag{11}$$

Stability is determined by linearizing this equation about $z = 0$:

$$\dot{z} = -z(t - T) + (3 - 2\alpha)z \tag{12}$$

Note that this is the same as Eq. (4) with α replaced by $3 - 2\alpha$. Thus, we use Eq. (9) to find the critical delay for Hopf bifurcation as:

$$T_H = \frac{\arccos(3 - 2\alpha)}{\sqrt{1 - (3 - 2\alpha)^2}} \tag{13}$$

Figure 3 shows the existence and stability of the equilibria located at $x = \pm\sqrt{\alpha - 1}$.

3 Limit cycles

We have seen in the foregoing that Eq. (2) exhibits various Hopf bifurcations, each generically yielding a limit cycle. We are concerned about the following questions regarding these limit cycles:

- (a) Are they stable, i.e., are the Hopf bifurcations supercritical?
- (b) What happens to the limit cycles after they are born in the Hopfs?

The question of the stability of the limit cycles may be answered by applying the multiple scales perturbation method to the nonlinear DDEs (2) and (11). In fact, this has already been accomplished in [7] for a general DDE of the form:

$$\begin{aligned} \frac{du}{dt} = & \gamma u + \beta u_d + a_1 u^2 + a_2 u u_d + a_3 u_d^2 + b_1 u^3 \\ & + b_2 u^2 u_d + b_3 u u_d^2 + b_4 u_d^3, \end{aligned} \tag{14}$$

where $u = u(t)$ and $u_d = u(t - T)$. The results of that reference are given in Appendix. When applied to Eq. (2), we find that the amplitude A of the limit cycle is given by the expression:

$$A^2 = \frac{-4(\alpha^2 - 1)^2}{3(\alpha\sqrt{1 - \alpha^2} \arccos \alpha + \alpha^2 - 1)} \mu, \tag{15}$$

where μ is the detuning off of the critical delay,

$$T = T_H + \mu, \tag{16}$$

and where the approximate form of the limit cycle is $x = A \cos \omega t$. Here, T_H and ω are given by Eqs. (8) and (9). A plot of the coefficient of μ in Eq. (15) is given in Fig. 4 for $-1 < \alpha < 1$. Note that this coefficient is nonnegative over this parameter range (cf. Fig. 2), which means that the limit cycle occurs for positive μ , i.e., for $T > T_H$, i.e., when the equilibrium at $x = 0$ is unstable. Since the Hopf occurs in a two-dimensional center manifold, this shows that the Hopf is supercritical and the limit cycle is stable.

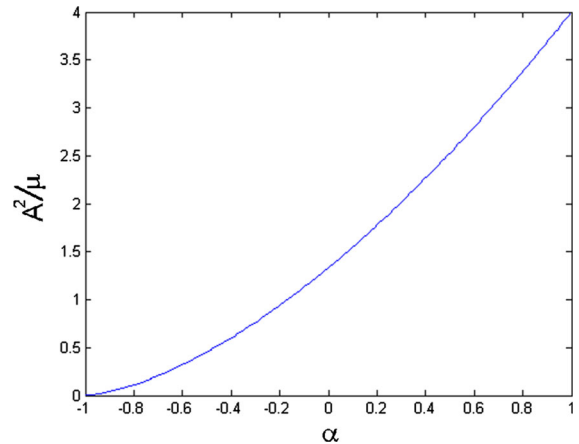


Fig. 4 Coefficient of μ in Eq. (15) is plotted for $-1 < \alpha < 1$. Its nonnegative value shows that the limit cycle is stable, see text

A similar analysis may be performed for limit cycles born from equilibria located on the arms of the pitchfork bifurcation. In this case, we use Eq. (11) and find that the limit cycle is unstable and that the Hopf is subcritical.

These results have been confirmed by comparison with numerical integration of Eq. (2) using the MATLAB function DDE23 and the continuation software DDE-BIFTOOL [8–10]. Figure 5 shows a limit cycle obtained using DDE23 for delay $T = 4$ and $\alpha = -0.75$. For these parameters, Eq. (9) gives $T_H = 3.6570$ and Eq. (15) gives a limit cycle amplitude of $A = 0.2312$. Also, Eq. (8) gives $\omega = 0.6614$, which gives a period of $2\pi/\omega = 9.4993$. Note that these computed values agree with the values obtained by numerical simulation in Fig. 5.

The DDE-BIFTOOL software shows that the limit cycles born in a Hopf from the equilibrium at $x = 0$ die in a limit cycle fold. Figure 6 displays two BIFTOOL plots of limit cycle amplitude ($\times 2$) versus α for $T = 1.1$ and $T = 3.5$. The collection of all such curves is a surface in $\alpha - T$ -amplitude space and is displayed in Fig. 7. Note that although the locus of limit cycle fold points cannot be found analytically, an approximation for it may be obtained from the DDE-BIFTOOL curves and is shown in Fig. 7. When projected down onto the $\alpha - T$ plane, it represents the boundary beyond which there are no stable limit cycles.

As noted above, the Hopf bifurcations off the equilibria located on the arms of the pitchfork are subcritical, i.e., the resulting limit cycle is unstable. This is

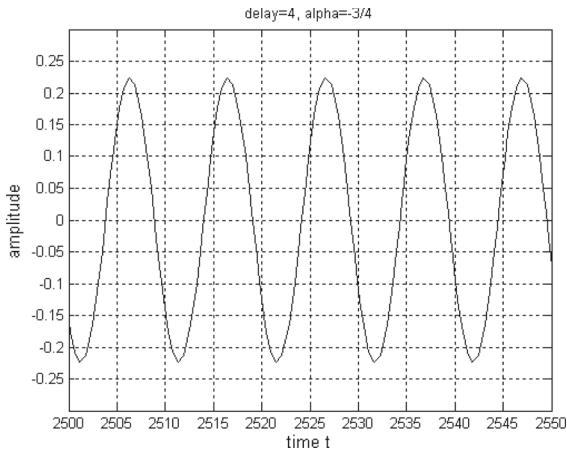


Fig. 5 Limit cycle obtained using DDE23 for delay $T = 4$ and $\alpha = -0.75$. The theoretical values of amplitude and period, namely $A = 0.2312$ and period = 0.6614 (see text), agree well with those seen in the simulation

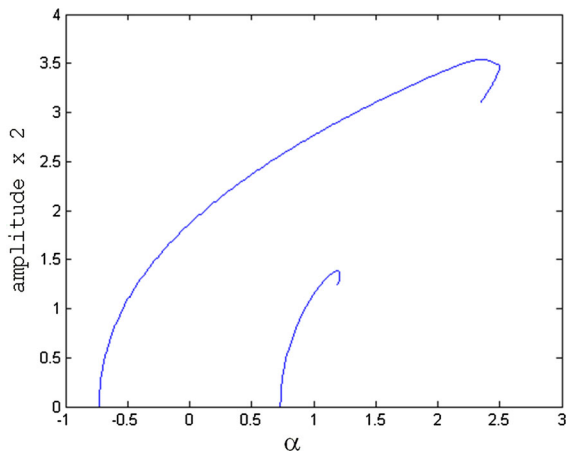


Fig. 6 BIFTOOL plots of limit cycle amplitude ($\times 2$) versus α . The *smaller curve* is for $T = 1.1$, and the *larger one* is for $T = 3.5$. Note that the limit cycles are born in a Hopf bifurcation and die in a limit cycle fold, i.e., by merging with an unstable limit cycle in a saddle-node bifurcation of cycles

illustrated in Fig. 8 which is a BIFTOOL computation showing the Hopf bifurcation at $\alpha = 1.5$ for varying delay T . Eq. (13) gives the critical value $T_H = \pi/2$.

4 Large delay

Numerical simulation of Eq. (2) shows that for large values of delay, the limit cycles take the form of an approximate square wave, see Fig. 9.

The following features have been observed in numerical simulations (cf. Fig. 9):

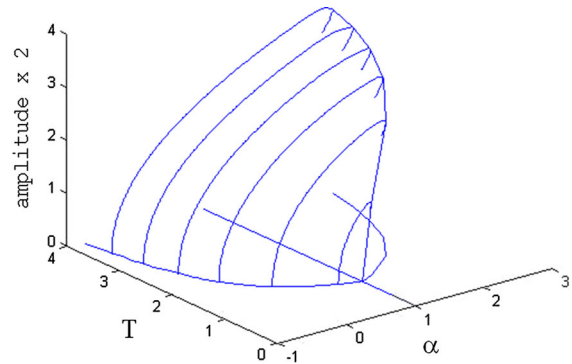


Fig. 7 A surface of limit cycles. Each limit cycle is born in a Hopf and dies in a limit cycle fold. The locus of limit cycle fold points is shown as a space curve and is also shown projected down onto the $\alpha - T$ plane

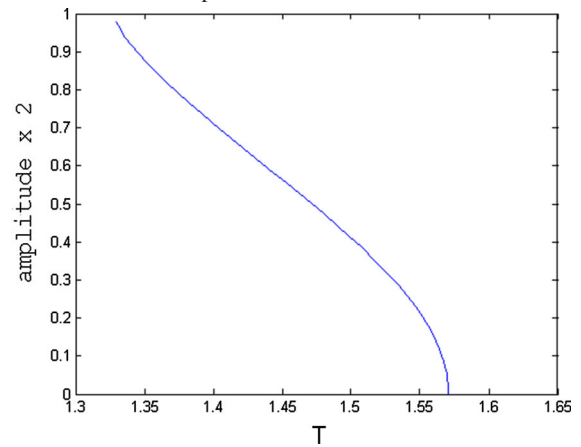


Fig. 8 BIFTOOL plot showing Hopf off the equilibrium at $x = \sqrt{\alpha - 1} = 0.7071$ for $\alpha = 1.5$, for varying delay T . Note that Eq. (13) gives the critical value $T_H = \pi/2$

1. The period of the square wave is approximately equal to twice the delay, $2T$.
2. The amplitude of the square wave is approximately equal to $\sqrt{1 + \alpha}$.
3. The large delay square wave is not found in simulations for which $\alpha > 3$.

In this section, we offer analytic explanations for these observations.

Since Eq. (2) is invariant under the transformation $x \mapsto -x$, we may refer to the value at the upper edge of the square wave as $x = A > 0$, in which case the value at the lower edge is $x = -A$. Then, at a point $x(t)$ on the lower edge, $x(t - T)$ refers to a point on the upper edge, $x(t - T) = A$, and Eq. (2) becomes

$$0 = -A - (-A)^3 + \alpha(-A) \tag{17}$$

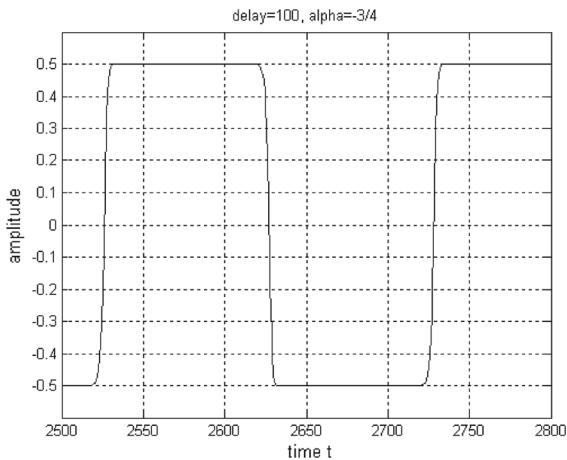


Fig. 9 Limit cycle obtained using DDE23 for delay $T = 100$ and $\alpha = -0.75$. Note the approximate form of a square wave, in contrast to the nearly sinusoidal wave shape for smaller values of delay, cf. Fig. 5

which gives the nontrivial solution

$$A = \sqrt{\alpha + 1} \tag{18}$$

Note that if $\alpha < -1$, this solution cannot exist, no matter what the delay T is.

During a jump down, $x(t - T)$ again takes on the value $\sqrt{\alpha + 1}$, so that (2) becomes

$$\frac{dx}{dt} = -\sqrt{\alpha + 1} - x^3 + \alpha x \tag{19}$$

Equation (19) has equilibria at

$$x = -\sqrt{\alpha + 1}, \quad x = \frac{\sqrt{\alpha + 1} \pm \sqrt{\alpha - 3}}{2} \tag{20}$$

For $\alpha < 3$, there is only one real root, $x = -A = -\sqrt{\alpha + 1}$.

During the jump down, the variable x starts at $\sqrt{\alpha + 1}$, which acts like an initial condition for the jump according to Eq. (19). The motion continues in x toward the equilibrium at $x = -\sqrt{\alpha + 1}$, which is approached for large time t . Note that the other two equilibria in Eq. (20) lie between $x = -\sqrt{\alpha + 1}$ and $x = \sqrt{\alpha + 1}$ in the case that $\alpha > 3$. Their presence prevents x from approaching $x = -\sqrt{\alpha + 1}$ and thus disrupts the jump, which explains why no square wave limit cycles are observed for $\alpha > 3$.

The foregoing argument assumes that the equilibrium at $x = -\sqrt{\alpha + 1}$ is stable. To investigate the stability of the equilibrium at $x = -\sqrt{\alpha + 1}$, we set

$$x = -\sqrt{\alpha + 1} + y \tag{21}$$

Substituting (21) into (19), we obtain

$$\frac{dy}{dt} = -y^3 + 3\sqrt{\alpha + 1}y^2 - (2\alpha + 3)y \tag{22}$$

Linearizing (22) for small y shows that $x = -\sqrt{\alpha + 1}$ is stable for $\alpha > -3/2$. Since the square wave solution ceases to exist when $\alpha < -1$, the restriction of $\alpha > -3/2$ is not relevant.

5 Discussion

In the foregoing sections, we have shown that the delay limit cycle oscillator with self-feedback, Eq. (2), supports a variety of dynamical phenomena, including Hopf and pitchfork bifurcations, limit cycle folds and relaxation oscillations. Numerical explorations using DDE-BIFTOOL have revealed that Eq. (2) exhibits many additional bifurcations, see, for example, Fig. 10.

We also note that due to the multivalued nature of arccosine, there are an infinite number of Hopf bifurcation curves in parameter space. Referring to Eqs. (9) and (13), these Hopf bifurcation curves can be generalized to:

$$T_H = \frac{(2\pi n + \arccos \alpha)}{\sqrt{1 - \alpha^2}} \tag{23}$$

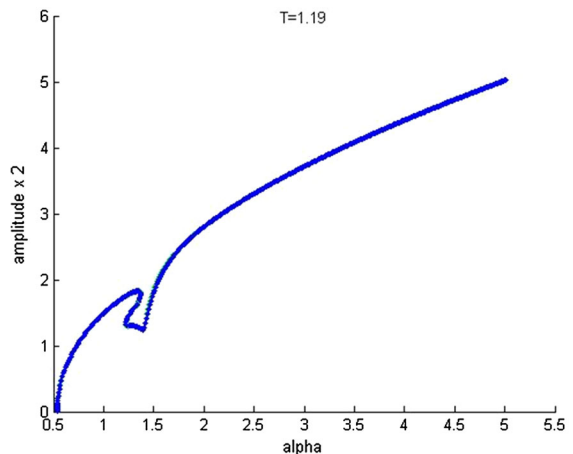


Fig. 10 Numerical simulation of Eq. (2) using DDE-BIFTOOL. Note that the left portion of the continuation curve is similar to those shown in Figs. 6 and 7. However, the additional bifurcations shown have not been identified. The periodic motions represented by the rest of the branch could not be found using DDE23 and are evidently unstable

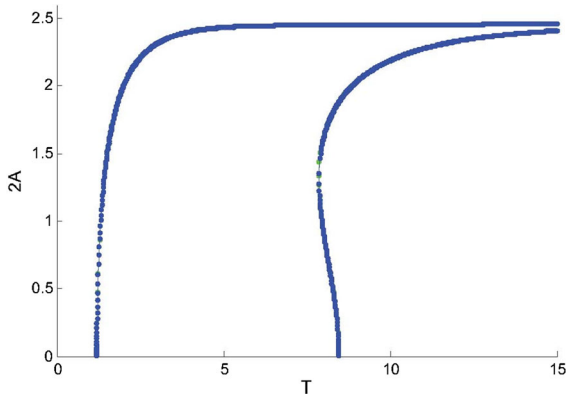


Fig. 11 DDE-BIFTOOL plots of the limit cycles created by the first two Hopf bifurcations at $x = 0$, found for $\alpha = 0.5$ and increasing T

$$T_H = \frac{(2\pi n + \arccos(3 - 2\alpha))}{\sqrt{1 - (3 - 2\alpha)^2}} \quad (24)$$

for integer n , where the $n = 0$ case represents the bifurcations already discussed. We use the principal value of arccos in this definition to be consistent with the original equations.

These additional bifurcations do not change the overall stability of the equilibria. The related periodic motions appear to be unstable and have not been observed in the results of DDE23 simulation. We can use numerical continuation in DDE-BIFTOOL to trace them for varying delay T ; for instance, Fig. 11 shows results for the motions created by the $n = 0$ and $n = 1$ Hopf bifurcations off of $x = 0$.

For large delay T , we found that square waves of higher frequency also existed. The periods of these higher-order square waves are given by $\frac{2T}{2n-1}$, where n is an integer and $n = 1$ corresponds to the base square wave previously analyzed. See, for example, Fig. 12, which shows a higher-order square wave for which $T = 100$, $\alpha = -0.75$ and $n = 2$.

Note that the amplitude of this square wave is the same as that of the base square wave, namely $A = \sqrt{\alpha + 1} = \sqrt{-0.75 + 1} = 1/2$. Note also that both the $n = 2$ higher-order square wave of Fig. 12 and the base square wave of Fig. 9 coexist, each of them corresponding to different initial conditions. In fact, higher-order square waves corresponding to larger values of n also coexist. An open question is what is the maximum value of n for which higher-order square waves exist? (The problem is that as n increases, the period

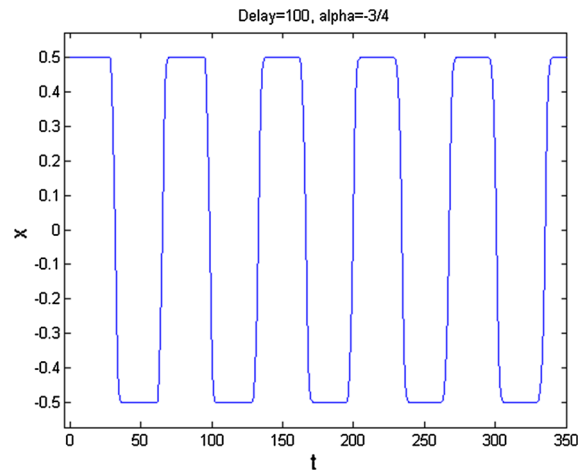


Fig. 12 A higher-order square wave for $T = 100$, $\alpha = -0.75$ and $n = 2$. Compare with the base square wave ($n = 1$) in Fig. 9

$\frac{2T}{2n-1}$ gets smaller, and the assumption that the period is large compared to the jump time is no longer valid.)

Each edge of the square wave has length equal to half the period, $\frac{T}{2n-1}$. An analysis similar to that presented above in the section on large delay, for the base case, can be repeated here.

6 Conclusions

In this work, we have shown that the diverse nature of the observed dynamics of the delay limit cycle oscillator with self-feedback, Eq. (2), depends on the values of the parameters T and α . This may be illustrated by reference to various regions of the $\alpha - T$ parameter plane. See Fig. 13, where the five regions *I, II, III, IV* and *V* are bounded by curves *a, b, c, d*.

Curve *a* is given by the Hopf condition Eq. (9), so that a stable limit cycle is born as we cross from region *I* to region *II*.

Curve *b* is simply $\alpha = 1$, and as we pass from region *II* to region *III*, a new pair of equilibrium points are born in a pitchfork bifurcation, see Fig. 1.

Curve *c* is given by the Hopf condition Eq. (13), so that an unstable limit cycle is born in a subcritical Hopf as we cross from region *III* to *IV*.

Curve *d* is a limit cycle fold, see Fig. 7. As we cross from region *IV* to region *V*, a stable limit cycle disappears in a fold. Thus, region *V* contains only the three equilibrium points, namely the origin (unstable) and the arms of the pitchfork (stable).

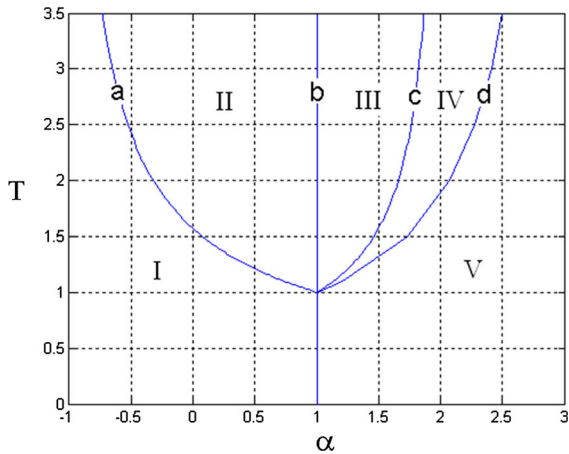


Fig. 13 Regions of $\alpha - T$ parameter space and the bifurcation curves which bound them

Finally, the pitchfork equilibria disappear as we cross from region V to region I.

In summary, we may list the stable dynamical structures which appear in the five regions as follows:

- Region I contains a stable equilibrium at the origin.
- Regions II and III contain a stable limit cycle (which was born in a Hopf off the origin).
- Region IV contains both a stable limit cycle and a pair of stable equilibria (the arms of the pitchfork).
- Region V contains a pair of stable equilibria (the arms of the pitchfork).

It is to be noted that the foregoing summary has omitted unstable motions (see Fig. 10) as well as motions occurring for large delay (see Figs. 9,12).

Equation (1), the basic delay limit cycle oscillator upon which this work is based [5,6], is perhaps the simplest example of a system which oscillates due to delay and nonlinearity. We look forward to further investigations based on this system.

Appendix: Hopf bifurcation formula for first-order DDEs

In this Appendix, we review the Hopf bifurcation formula, first derived in [7], for first-order constant-coefficient differential-delay equations of the form of Eq. (14). The amplitude A of the approximate solution $u = A \cos \omega t$ is given by the expression:

$$A^2 = \mu P/Q, \tag{25}$$

where

$$\begin{aligned}
 P &= 4\beta^3(4\gamma - 5\beta)(\beta - \gamma)(\gamma + \beta)^2 \tag{26} \\
 Q &= 5b_2T_H\beta^6 + 15b_4T_H\beta^6 + 15b_1\beta^5 + 5b_3\beta^5 - 4a_1^2T_H\beta^5 \\
 &\quad - 3a_2^2T_H\beta^5 - 22a_3^2T_H\beta^5 - 7a_1a_2T_H\beta^5 - 14a_1a_3T_H\beta^5 \\
 &\quad - 7a_2a_3T_H\beta^5 - 15\gamma b_1T_H\beta^5 + \gamma b_2T_H\beta^5 - 15\gamma b_3T_H\beta^5 \\
 &\quad + 3\gamma b_4T_H\beta^5 - 18a_1^2\beta^4 - a_2^2\beta^4 - 4a_3^2\beta^4 - 9a_1a_2\beta^4 \\
 &\quad - 18a_1a_3\beta^4 - 9a_2a_3\beta^4 + 3\gamma b_1\beta^4 - 15\gamma b_2\beta^4 + \gamma b_3\beta^4 \\
 &\quad - 15\gamma b_4\beta^4 + 18\gamma a_1^2T_H\beta^4 + 7\gamma a_2^2T_H\beta^4 + 12\gamma a_3^2T_H\beta^4 \\
 &\quad + 19\gamma a_1a_2T_H\beta^4 + 30\gamma a_1a_3T_H\beta^4 + 37\gamma a_2a_3T_H\beta^4 \\
 &\quad - 3\gamma^2b_1T_H\beta^4 + 6\gamma^2b_2T_H\beta^4 - 3\gamma^2b_3T_H\beta^4 \\
 &\quad - 12\gamma^2b_4T_H\beta^4 \\
 &\quad + 12\gamma a_1^2\beta^3 + 11\gamma a_2^2\beta^3 + 26\gamma a_3^2\beta^3 + 33\gamma a_1a_2\beta^3 \\
 &\quad + 30\gamma a_1a_3\beta^3 + 19\gamma a_2a_3\beta^3 - 12\gamma^2b_1\beta^3 - 3\gamma^2b_2\beta^3 \\
 &\quad + 6\gamma^2b_3\beta^3 - 3\gamma^2b_4\beta^3 - 8\gamma^2a_1^2T_H\beta^3 - 12\gamma^2a_2^2T_H\beta^3 \\
 &\quad + 4\gamma^2a_3^2T_H\beta^3 - 26\gamma^2a_1a_2T_H\beta^3 - 16\gamma^2a_1a_3T_H\beta^3 \\
 &\quad - 20\gamma^2a_2a_3T_H\beta^3 + 12\gamma^3b_1T_H\beta^3 + 2\gamma^3b_2T_H\beta^3 \\
 &\quad + 12\gamma^3b_3T_H\beta^3 - 14\gamma^2a_2^2\beta^2 - 8\gamma^2a_3^2\beta^2 - 18\gamma^2a_1a_2\beta^2 \\
 &\quad - 12\gamma^2a_1a_3\beta^2 - 32\gamma^2a_2a_3\beta^2 + 12\gamma^3b_2\beta^2 + 2\gamma^3b_3\beta^2 \\
 &\quad + 12\gamma^3b_4\beta^2 + 8\gamma^3a_2^2T_H\beta^2 + 8\gamma^3a_1a_2T_H\beta^2 \\
 &\quad - 4\gamma^3a_2a_3T_H\beta^2 - 8\gamma^4b_2T_H\beta^2 + 4\gamma^3a_2^2\beta \\
 &\quad - 8\gamma^3a_3^2\beta + 8\gamma^3a_2a_3\beta - 8\gamma^4b_3\beta + 8\gamma^4a_2a_3, \tag{27}
 \end{aligned}$$

where ω and T_H are the values of frequency and delay associated with the Hopf and where $\mu = T - T_H$.

In the case of the delay limit cycle oscillator with self-feedback, Eq. (2), we have for the Hopf at $u = x = 0$:

- $\gamma = \alpha$
- $\beta = -1$
- $a_1 = a_2 = a_3 = 0$
- $b_1 = -1$
- $b_2 = b_3 = b_4 = 0$

and we have T_H given by Eq. (9). When these parameter values are substituted into the above expressions for P and Q , we obtain Eq. (15).

References

1. Rayleigh, L.: The Theory of Sound, p. 81. Dover Publications, Mineola (1945)
2. van der Pol, B.: On "relaxation-oscillations". Lond. Edinb. Dublin Philosoph. Mag. J. Sci. Ser. 7 2, 978–992 (1926)
3. Suchorsky, M.K., Sah, S.M., Rand, R.H.: Using delay to quench undesirable vibrations. Nonlinear Dyn. 62, 407–416 (2010)

4. Atay, F.M.: Van der Pol's oscillator under delayed feedback. *J. Sound Vib.* **218**(2), 333–339 (1998)
5. Rand, R.H.: Lecture notes in nonlinear vibrations published on-line by the Internet-First University Press <http://ecommons.library.cornell.edu/handle/1813/28989> (2012)
6. Rand, R.: Differential-delay equations. In: Luo, A.C.J., Sun, J.-Q. (eds.) Chapter 3 in “Complex Systems: Fractionality, Time-delay and Synchronization”, pp. 83–117. Springer, Berlin (2011)
7. Verdugo, A., Rand, R.: Hopf bifurcation formula for first order differential-delay equations. *Commun. Nonlinear Sci. Numer. Simul.* **12**, 859–864 (2007)
8. Engelborghs, K., Luzyanina, T., Roose, D.: Numerical bifurcation analysis of delay differential equations using: DDE-BIFTOOL. *ACM Trans. Math. Softw.* **28**(1), 1–21 (2002)
9. Engelborghs, K., Luzyanina, T., Samaey, G.: DDE-BIFTOOL v. 2.00: a Matlab package for bifurcation analysis of delay differential equations. Technical Report TW-330, Dept. Comp. Sci., K.U.Leuven, Leuven, Belgium (2001)
10. Heckman, C.R.: An introduction to DDE-BIFTOOL is available as Appendix B of the doctoral thesis of Christopher Heckman: asymptotic and numerical analysis of delay-coupled microbubble oscillators (Doctoral Thesis). Cornell University (2012)